LANGMUIR

pubs.acs.org/Langmuir Article

Separation of Perfluorooctanoic Acid from Water Using Meso- and Macroporous Syndiotactic Polystyrene Gels

Pratik S. Gotad, Calum Bochenek, Chrys Wesdemiotis, and Sadhan C. Jana*

Cite This: *Langmuir* 2024, 40, 10208−10216 Read Online

ACCESS | Metrics & More | Article Recommendations | Supporting Information

ABSTRACT: Per- and polyfluoroalkyl substances are an emerging class of contaminants that are environmentally persistent, bioaccumulative, and noxious to human health. Among these, perfluorooctanoic acid (PFOA) molecules are widely found in ground and surface water sources. A novel high surface area, meso- and macroporous syndiotactic polystyrene (sPS) wet gel is used in this work as the adsorbent of PFOA molecules from water at environmentally relevant PFOA concentrations (≤1 μg/L) and cleanse water to below the U.S. EPA's 2023 health advisory limit of 4 parts per trillion (ppt). The sigmoidal shape of the PFOA adsorption isotherm indicates a two-step adsorption mechanism attributed to the strong affinity of PFOA molecules for the sPS surface and molecular aggregation at solid−liquid interfaces or within the pores of the sPS wet gel. The adsorption kinetics and the effects of sPS wet gel porosity, pore size, and pore volume on the removal efficiency are reported. The adsorption kinetics is seen to be strongly dependent on pore size and pore volume.

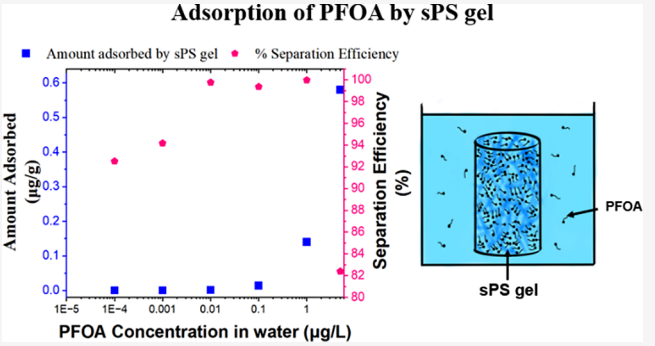

INTRODUCTION

Per- and polyfluoroalkyl substances (PFAS) are a group of manmade chemicals that are recognized as contaminants of emerging concern due to their toxicity, bioaccumulation, and ability to persist in the environment for a long period of time, largely due to their extremely stable carbon−fluorine bonds, thereby receiving the notoriety as "forever chemicals".[1,2] A large-scale contamination of ground and surface water sources by these chemicals has prompted United States Environmental Protection Agency (EPA) to list them among top priority contaminants.[3] An estimated 110 million people in the United States alone are exposed to PFAS-contaminated drinking water.[4] A number of prior studies linked PFAS accumulation in human bodies to certain types of cancers, liver damage, reduced immune response, negative impact on the reproductive system such as reduced fertility, birth defects, and many more health issues.[3,5,6] In addition, the negative ecological impact of these chemicals on the aquatic ecosystem is also a concern.[7] Therefore, addressing the removal of PFAS from water streams is the growing need of the hour.

PFAS are used in large-scale manufacturing of poly(tetrafluoroethylene) (Teflon) and in numerous everyday consumer products such as food packaging, clothing, coatings, and menstrual products, to name a few.[1,8] The US EPA identified around 430 PFAS molecules obtained from various water sources and included 74 chemicals in the top priority list targeted for obtaining additional toxicity data.[9,10] However, certain types of PFAS molecules, namely, perfluorooctanoic acid (PFOA), perfluorooctanesulfonic acid (PFOS), perfluorobutanoic acid (PFBA), perfluorobutanesulfonic acid (PFBS), and GenX chemicals, came under stringent scrutiny due to their widespread use and proven adverse impacts on human health.[11−13] In 2022, the US EPA assigned a health advisory limit for PFOA of 0.004 ng/L and for PFOS of 0.02 ng/L compared to the previously set limit in 2016 of 70 ng/L for both these compounds.[11,14] In view of the above stringent advisory limits, this work addressed high efficiency separation of perfluorooctanoic acid (PFOA), the most widespread PFAS contaminant present in the environment, using novel mesoporous−macroporous adsorbent media.

Several techniques such as chemical oxidation,[15] foam fractionation,[16] coagulation,[17] ion exchange,[18] and filtration[19] were studied for PFOA removal or degradation. However, the most viable and commercially scalable technology involves the use of natural or synthetic adsorbent media due to their greater effectiveness for the separation of PFOA molecules compared to other available technologies. A few of the adsorbents considered as the frontrunners in terms of their performance are granular/powdered activated carbon,[20−22] amine-containing compounds,[13,23] biochar,[24] and ion-exchange resins.[25]

Received: February 7, 2024
Revised: April 20, 2024
Accepted: April 22, 2024
Published: May 2, 2024

https://doi.org/10.1021/acs.langmuir.4c00482
Langmuir 2024, 40, 10208−10216

However, a few known drawbacks limit the performance of these adsorbents in PFOA separation.[1] For example, activated carbon is inexpensive, but it suffers from poor adsorption of PFOA at environmentally relevant concentrations (≤1 μg/L), long adsorption times, low effectiveness for short-chain PFAS molecule separation, poor performance in the presence of other organic contaminants, and difficulty in regeneration of the adsorbent bed for sustainable use. In the same vein, a majority of adsorption media, such as β-cyclodextrin (β-CD)[13] and ion-exchange resins,[25] offer extremely low specific surface area and hence low adsorption capacities, thus requiring frequent regeneration of the adsorbent bed. In addition, ion-exchange resins are highly selective toward either anionic or cationic PFAS. Their performance in separation of nonionic molecules is poor, and their effectiveness for PFAS separation in the presence of other salts in water is low.[1]

Most importantly, the majority of adsorbent materials reported in literature were not associated with the separation of PFOA at the desired low concentrations (≤1 μg/L), thus limiting their effectiveness for the separation task.[23] To the best of our knowledge, none of the currently available adsorbent materials can meet the April 2024 EPA guidelines for enforceable levels of PFOA concentration (4 ng/L or 4 ppt). In this context, novel adsorbent media are needed that offer high adsorption potential for PFOA at environmentally relevant concentrations, such as high adsorption capacity, rapid adsorption kinetics, and inexpensive regeneration, to address the emerging stringent environmental limits and the ensuing health hazards that these molecules present. The above issues were addressed in this work by considering mesoporous and macroporous polymer wet gels, specifically syndiotactic polystyrene (sPS) wet gels, as the adsorbent for the separation of PFOA molecules from water initially available at an industrially relevant concentration of ≤1 μg/L.

Polymer gels offer a high surface area (200−1000 m^2/g),[26−28] a high pore volume (>90%),[29−32] and an interconnected network of abundant mesopores (2−50 nm) and macropores (>50 nm). The pore-filling liquid in the polymer gels can be easily replaced by a gas in the supercritical drying step to obtain aerogels.[33] Aerogels can be rendered into various shapes and sizes such as monoliths,[34] sheets,[35,36] films,[37] and spherical[27,38] or pill-shaped[39] microparticles. The pore size and surface energy of the materials can also be tuned for desired applications.[26,40−42] The development of this class of materials over 90 years led to several high value innovations in thermal insulation,[43] air filtration,[44−46] energy storage,[47] molecular separation,[28,39] and filtration.[48]

An earlier study established high adsorption capacity of three polymer wet gels, namely, sPS, polyimide, and polyurea, for the removal of a nonionic, triblock copolymer surfactant poly(ethylene oxide) (PEO)-poly(propylene oxide) (PPO)-PEO from solutions in water.[28] An adsorption capacity of around 2−3 g/g was achieved in the case of the sPS wet gels. Such adsorption capacities are unusually high in reference to the data available for other porous materials[49−52] and are attributed to high surface energy and high specific surface area of sPS gels. sPS aerogels were first reported in 2005 by Daniel et al.[53] The high specific surface area, large porosity, and hydrophobic surface made these materials suitable for applications as adsorbents,[28] absorbents,[54,55] in oil−water separation,[56] and as a ultra- low dielectric constant material.[57]

The present work investigated adsorption kinetics and separation efficiency of PFOA molecules by sPS wet gels starting at environmentally relevant concentrations ≤1 μg/L in water. The effects of the polymer gel pore volume and surface area on adsorption performance were analyzed. Most known adsorbents have low specific surface areas, and these materials reach saturation adsorption limits quickly. Consequently, these materials can be reused only after regeneration by conducting the desorption of PFOA molecules. As will be seen later, the sPS wet gels considered in this work had a high specific surface area attributed to polymer strands of typical diameter 50 nm that offer many adsorption sites and hence a high adsorbent saturation capacity. To demonstrate this attribute, PFOA-loaded sPS wet gels obtained from one set of experiments were subjected to additional adsorption cycles in PFOA−water solution, and the ability of the wet gel to remove additional PFOA molecules was investigated. The findings reported in this work demonstrate the strong promise of the sPS wet gel for the removal of PFAS molecules from their solutions in water.

EXPERIMENTAL SECTION

Materials. Syndiotactic polystyrene (M_w ≈ 300,000 g/mol, 98%) was procured from Scientific Polymer Producers Inc. (Ontario, NY, U.S.A.). Toluene was purchased from Sigma-Aldrich (Milwaukee, WI, U.S.A). Ethanol was purchased from Decon Laboratories Inc. (King of Prussia, PA, U.S.A.). Perfluorooctanoic acid (PFOA, 96%) and perfluoroheptanoic acid (purity ≥98.0%, used as an internal standard) were purchased from Sigma-Aldrich (Milwaukee, WI, U.S.A). All chemicals were used as received without further purification.

Fabrication of sPS Polymer Wet Gels and Aerogels. sPS gels were obtained by thermoreversible gelation of solutions of sPS in toluene. sPS solutions were prepared with solid concentrations of 0.02, 0.06, and 0.08 g/mL by dissolving sPS in toluene in sealed vials at 100 °C and allowing solutions to cool under ambient conditions for 1 min followed by pouring into a covered cylindrical glass mold with 15 mm diameter for gelation. The gels were allowed to stand in the mold for 5 h to ensure complete gelation and were demolded, and the solvent was exchanged first with ethanol and finally with deionized (DI) water to obtain water-filled sPS wet gels. To obtain sPS aerogels, the ethanol-filled sPS gels were solvent-exchanged with liquid carbon dioxide and dried under supercritical conditions of carbon dioxide at 50 °C and 11 MPa pressure to recover sPS aerogels. The aerogels were used for BET surface area measurement and for examining morphology using a scanning electron microscope.

Characterization. *Porosity, Skeletal Density, and Bulk Density.* Helium pycnometer (AccuPyc II 1340, Micromeritics Instrument Corp., Norcross, GA) was used to obtain skeletal density (ρ_s). The bulk density (ρ_b) was obtained from the weight and volume of cylindrical aerogel monolith specimens. The bulk and skeletal density yielded total porosity (Π_T) and total pore volume (V_{total}) of the aerogels as expressed in eqs 1 and 2, respectively.

$$\Pi_T = (1 - \rho_b/\rho_s) \times 100 \quad (1)$$

$$V_{total} = \frac{1}{\rho_b} - \frac{1}{\rho_s} \quad (2)$$

Specific Surface Area and Pore Size Analysis. The Brunauer−Emmett−Teller (BET) adsorption−desorption analysis was used to obtain a specific surface area and mesopore volume (V_{meso}) of sPS aerogels. A Micromeritics Tristar II 3020 analyzer (Micromeritics Instrument Corp., Norcross, GA) was used for this purpose to obtain N_2 adsorption−desorption isotherms at 77 K. The nonlocal density functional theory (NLDFT) model was used to obtain the mesopore volume fraction from N_2 isotherms at 77 K. The macropore (diameter >50 nm) volume (V_{macro}) was obtained from the difference between the total pore volume (V_{total}, eq 2) and the mesopore volume (V_{meso}). The fractions of meso- (ϕ_{meso}) and macropores (ϕ_{macro}) were calculated using eqs 3 and 4.

https://doi.org/10.1021/acs.langmuir.4c00482
Langmuir 2024, 40, 10208−10216

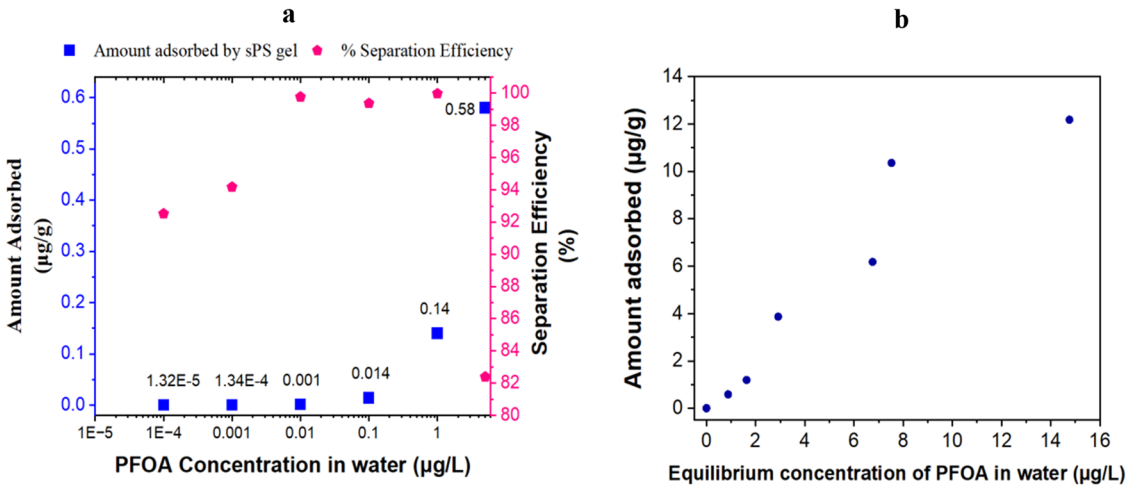

Figure 1. (a) Blue: Amount of PFOA adsorbed (μg/g) as a function of PFOA concentration in water (at and below environmentally relevant concentrations), Pink: % separation efficiency as a function of PFOA concentration in water, (b) adsorption isotherm, amount adsorbed by sPS gel vs the equilibrium concentration of PFOA in water (sPS wet gel dimensions: diameter 1.5 ± 0.1 cm and height 0.85 ± 0.02 cm).

$$\phi_{meso} = \frac{V_{meso}}{V_{total}} \quad (3)$$

$$\phi_{macro} = \frac{V_{macro}}{V_{total}} = 1 - \phi_{meso} \quad (4)$$

Morphology. The morphology of aerogel specimens was examined using a scanning electron microscope (SEM JSM5310, JEOL, MA).

Mass Spectrometry Analysis of PFOA in Water. Electrospray ionization mass spectrometry (ESI-MS) experiments were performed on a Bruker timsTOF Pro 2 (Bruker Daltonics, Billerica, MA). Solutions of PFOA in Millipore/DI H_2O at various concentrations were diluted with MeOH containing the internal standard, perfluoroheptanoic acid (PFHA), at a concentration of 5.0 ng/mL. The final 1:1 H_2O/MeOH (v/v) working solutions were then filtered using a Supor Membrane 0.1 μm Filter (Pall Corporation, Port Washington, NY), and the concentration of each analyte was determined by using the internal standard technique. The solutions were introduced into the ESI source via direct injection and electrospraying at a flow rate of 5 μL/min. The end plate and capillary voltages were set to 400 V and 4.5 kV, respectively, while the nebulizing gas (N_2) pressure and drying gas flow rate and temperature were set at 1.5 bar, 4 L/min, and 300 °C, respectively. The PFOA and PFHA ions were identified at $m/z \sim 368.9$ and 318.9, respectively. All data were acquired in triplicate via the MS scan mode with the instrument settings as follows: deflection 1 delta: −80 V, funnel 1 RF: 350 Vpp, isCID energy: 0 eV, funnel 2 RF: 300 Vpp, multipole RF: 300 Vpp, transfer time: 65 μs, and prePulse storage: 5 μs. The DataAnalysis 6.1 program (BrukerDaltonics, Bremen, Germany) was used for postacquisition data processing.

PFOA Adsorption Experiments. The amount of PFOA present in water was determined using a mass spectrometry technique mentioned in the above section and a calibration curve (Figures S1 and S2). The adsorption isotherm was obtained using PFOA solutions of concentrations ranging from 0.0001 to 100 μg/L. These solutions were prepared by serially diluting a stock solution of 10 mg/L PFOA. A representative sPS wet gel of known solid mass and cylindrical shape of diameter 1.5 ± 0.1 cm and height 0.85 ± 0.02 cm was dipped in PFOA solutions for 24 h. The amount of PFOA adsorbed by the sPS wet gel was obtained by determining the initial (C_0) and final (C_1) PFOA concentrations in water. The adsorbed quantity was converted to the mass of PFOA adsorbed (μg)/solid mass of sPS (g). The separation efficiency was obtained by using eq 5.

$$\%\ \text{Separation efficiency} = \frac{C_0 - C_1}{C_0} \times 100 \quad (5)$$

For obtaining the adsorption kinetics data, a representative sPS wet gel, obtained with 0.06 g/mL sPS concentration, was dipped in a 10 mL solution of 1 μg/L PFOA and taken out after a predetermined exposure time. The amount of PFOA in the residual water was determined. These experiments were repeated using a fresh wet gel and a new 10 mL solution of PFOA for various exposure times in the range of 5−1440 min. The separation efficiency was obtained using eq 5. Experiments were performed three times for each exposure time.

RESULTS AND DISCUSSION

PFOA Adsorption Isotherm and Adsorption Kinetics by sPS Gel. The PFOA adsorption isotherms were generated by dipping a wet gel obtained from 0.06 g/mL sPS solid concentration into 10 mL of PFOA solutions of concentrations ranging from 0.0001 to 100 μg/L for 24 h. It should be noted that the environmentally relevant concentration of PFOA in water is considered by prior researchers as 1 μg/L.[23] It will be seen later that a dipping time of 24 h was more than adequate for reaching an equilibrium. The adsorption isotherm was generated with PFOA concentrations well below and above this concentration. Figure 1a (blue) depicts the amount of PFOA adsorbed by the sPS gel in μg/g as a function of PFOA initial concentration in water. A sPS wet gel with a solid weight of 70 mg was used for these experiments.

The first striking observation is the shape of the adsorption isotherm curve presented in Figure 1b, where the equilibrium concentrations of PFOA in water are plotted against the amounts of PFOA adsorbed by the wet gel. The data trend is approximately sigmoidal (S-shaped; Figure 1b) with an inflection point at around 2 μg/L, indicating aggregation or multilayer adsorption of molecules on the adsorbent surface. The structural aggregation of the PFOA molecules can occur in one of the following manners—bilayers,[58] hemimicelles,[59] micelles,[60] or other forms. Such adsorption curves suggest a strong affinity between the adsorbate and adsorbent and also between the adsorbed and nonadsorbed molecules.[49,61] At the highest initial PFOA concentration of 100 μg/L, the amount of PFOA adsorbed by the gel was ∼12.17 μg/g, and the equilibrium concentration of PFOA in the liquid was 14.76 μg/L. However, this should not be mistaken to be the maximum adsorption capacity of the gel since a plateau or saturation in the adsorbed amount cannot be ascertained at this concentration. PFOA concentrations higher than 100 μg/

https://doi.org/10.1021/acs.langmuir.4c00482
Langmuir 2024, 40, 10208−10216

L in water were not considered in this work. A thorough study will be separately conducted to discover the adsorption regimes at concentrations higher than 100 μg/L.

The second important observation from the data presented in Figure 1 is the trend of the separation efficiency data as a function of the bulk PFOA concentration (Figure 1a, pink data points). At the environmentally relevant concentration of 1 μg/L, the separation efficiency of the sPS gel was found to be 99.98 ± 0.01%, achieved in ∼24 h. The PFOA concentration in water after adsorption by the sPS gel decreased to about 0.2 ng/L or 0.2 ppt in 24 h. In this context, a limited number of adsorbents such as β-cyclodextrin polymer (∼99% separation efficiency in 24 h), polyethylenimine-functionalized cellulose microcrystals (∼90−95% separation efficiency in 16 h), and aminated β-cyclodextrin (∼99% separation efficiency in 9 h) produced such high separation performance for PFOA.[13,62−65] To support the above observation, a set of benchmarking experiments were conducted using two commercially available adsorbents used in PFAS removal, such as activated carbon and ion-exchange resins, respectively, in the form of Calgon F-400 and ion-exchange resin in Zero Water filters. The test solutions contained PFOA at a 1 μg/L concentration in water. The specific surface area of activated carbon and ion-exchange resin was measured using BET to be 730 and 80 m^2/g. The BET adsorption−desorption isotherms for the two materials are shown in Figures S3 and S4. The solid weight of each adsorbent was adjusted to obtain a total surface area of 30 m^2/g for all three adsorbents−sPS wet gel, activated carbon, and ion-exchange resin. The activated carbon and the ion-exchange resin showed a separation efficiency of 81.10 ± 0.2 and 43.10 ± 1.12%, respectively, compared to the separation efficiency of 99.98 ± 0.01% for the sPS wet gel.

In addition, most adsorbents, such as activated carbon, take hours or even days to reach >90% separation efficiency.[1,66] The slow adsorption kinetics in the case of activated carbons is attributed to the small pore size, which is predominantly microporous (<2 nm), thereby limiting the diffusion ability of the PFOA molecules with typical size˜ 2 nm. The third aspect to notice here is the adsorption performance of the sPS gel at PFOA concentrations lower than 1 μg/L.

It was observed that the sPS wet gel considered in this work showed a separation efficiency of >90% for all PFOA concentrations below 1 μg/L. Specifically, the values of separation efficiency were 92.5, 94.1, 99.7, and 99.3% for PFOA concentrations of, respectively, 0.0001, 0.001, 0.01, and 0.1 μg/L. We attribute this trend to the cooperative functioning of the diffusive flux of the surfactant from the bulk into the pores of sPS gel and the adsorption kinetics of the surfactant on polymer strand surfaces inside the gel. The use of a finite-size gel specimen of diameter 1.5 ± 0.1 cm and height 0.85 ± 0.02 cm did not allow all surfactant molecules present in the bulk to access high surface area polymer strands present inside the pores. The surfactant molecules must diffuse from the bulk to the macroscopic gel specimen surface, diffuse through the pores to access high surface area polymer strands, and finally adsorb onto the polymer surfaces. The favorable interactions between sPS polymer strand surfaces in the wet gel and the PFOA molecules that diffused into the pores potentially led to thermodynamically stable structural configuration and aggregation of PFOA molecules on the adsorbent surface as was noted by Shin et al.[49] for a set of surfactant−silica systems. This in turn promotes further molecular diffusion from the bulk to the pores and from the water phase inside the pores onto solid sPS strands. A thorough characterization of PFOA aggregation on sPS strand surfaces, however, is needed to support an analogy with the work of Shin et al.[49]

At lower PFOA concentrations of 0.0001 and 0.001 μg/L, the concentration gradients across the bulk liquid and within the sPS gel were much smaller, respectively, 2 and 1 order of magnitude compared to a PFOA concentration of 0.01 μg/L. Accordingly, the slower diffusion flux controlled the adsorption performance at lower concentrations. The diffusive flux increased at higher PFOA concentration in the bulk liquid, leading to quicker diffusion and adsorption of molecules. In this work, adsorption experiments were performed for 24 h. It is conceivable that only a part of the available sPS gel surface was covered, yielding a lower separation efficiency. The data presented in Figure 1a support that sPS wet gels are very effective in removing PFOA even when present in extremely low concentrations.

One can also quantify the adsorption performance in terms of an effective concentration (C_{eff}) of the adsorbed PFOA molecules within the sPS gel as a function of bulk concentration (C_{bulk}). Such data are shown in Figure 2. The

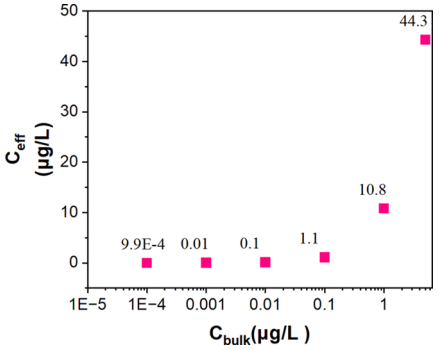

Figure 2. Effective concentration of adsorbed PFOA within the sPS gel (0.06 g/mL solid concentration) as a function of the PFOA concentration in water.

value of C_{eff} within the wet gel was calculated from the mass of PFOA adsorbed by the gel and the volume of water needed to fill all of the pores of the gel. As an example, the effective concentration of PFOA within the sPS gel dipped in a 0.01 μg/L PFOA solution was calculated from the weight of the sPS wet gel, e.g., 1 g of sPS, and its porosity of 93% (Table 1). This gel had 93% of its volume occupied by water, accounting for 0.93 g of water and 0.07 g of sPS. The amount of PFOA adsorbed by this sPS wet gel was 0.014 μg/g of solid sPS

Table 1. Bulk Density, Skeletal Density, Porosity, Pore Volume, Surface Area, and Mesomacropore Volume Fraction of sPS Polymer Aerogels[a]

sPS solid concentration (g/mL)	bulk density (ρ_b; g/cm^3)	total porosity (Π_T) (%)	BET surface area (m^2/g)	V_{Total} (cm^3/g)	ϕ_{meso}; ϕ_{macro}
0.02	0.031 ± 0.001	97.1	313 ± 7	31.3	0.02; 0.98
0.06	0.080 ± 0.003	93	296 ± 15	11.5	0.06; 0.94
0.08	0.105 ± 0.004	90	280 ± 10	8.6	0.07; 0.93

[a]sPS skeletal density (ρ_s): 1.05 g/cm^3.

https://doi.org/10.1021/acs.langmuir.4c00482
Langmuir 2024, 40, 10208−10216

(Figure 1a). Accordingly, the value of C_{eff} was (0.014 μg/g)(0.07 g)/(0.00093 L), or 1.1 μg/L, indicating that C_{eff} was approximately 11 times higher than C_{bulk} for an initial bulk concentration of 0.1 μg/L. A value of $C_{eff} \gg C_0$ indicates effective separation.

An earlier study by Gotad et al.[28] underlined the role of high interfacial energy sPS−water interfaces in driving the adsorption of block copolymer surfactants within the water-filled sPS gel. The amount of surfactant adsorbed scaled directly with the interfacial energy. A similar argument can be invoked in this work to explain the driving force for PFOA adsorption on sPS gels in view of the similar molecular structure of the PFOA molecules to that of the surfactant considered by Gotad et al.,[28] with a hydrophilic −COOH group at one end and the 8-carbon long chain with fluorine groups at the other.

Another important parameter determining the effectiveness of an adsorbent is the kinetics of the adsorption of PFOA molecules from a solution in water. Figure 3 shows a representative plot showing separation efficiency as a function of time for the removal of PFOA using sPS gel produced from 0.06 g/mL sPS solution in toluene. In this case, cylindrical monolithic sPS wet gel (diameter 1.5 ± 0.1 cm and height 0.85 ± 0.02 cm) specimens of approximately 70 mg solid weight were dipped in a 1 μg/L PFOA solution in water over a period of 24 h.

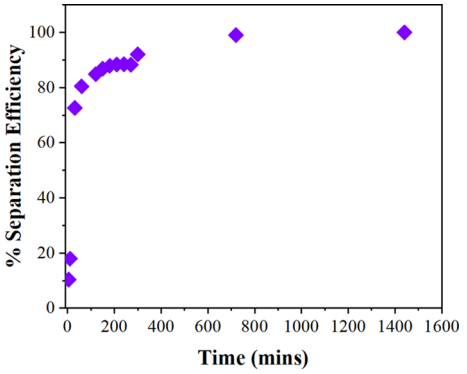

Figure 3. Time-dependent PFOA adsorption by sPS wet gels obtained from the sPS solution of 0.06 g/mL solid concentration from 1 μg/L PFOA solutions in water. sPS wet gel dimensions: diameter 1.5 ± 0.1 and height 0.85 ± 0.02 cm.

It is noted from prior work that the kinetics of adsorption are largely governed by the adsorbent pore size, adsorbent amount, and the shape of the adsorbent.[24,67,68] It is seen from Figure 3 that PFOA adsorption was fast at the beginning and reached an asymptote at a later period. For example, it took ∼5 h (300 min) to reach 92% separation efficiency and ∼12 and 24 h to attain separation efficiencies of 98.99 and 99.98%, respectively. A steep rise in adsorption was observed in the 5−30 min interval; e.g., the separation efficiency increased from ∼10% at 5 min to ∼72% at 30 min. Such a steep rise in the adsorption behavior indicates fast diffusion of PFOA molecules within the sPS gels and their subsequent fast adsorption onto the sPS surface. As will be illustrated later, faster adsorption kinetics can be achieved via manipulation of the pore sizes and pore volumes offered by the gel, achieving >90% separation in an hour.

Effect of sPS Gel Pore Volume and Specific Surface Area on PFOA Adsorption. In this section, the effects of the sPS concentration in the gel on the adsorption performance of PFOA molecules are discussed. sPS gels were prepared from 0.02, 0.06, and 0.08 g/mL sPS in toluene, producing specimens with different values of total porosity (Π_T), pore size, and specific surface area. Such data and the values of the bulk and skeletal density are presented in Table 1.

A higher solid polymer concentration in the gel results in an increase in the sPS strand diameter and a reduction of the pore size and pore volume of the gel (Table 1). The sPS aerogels showed a porosity of ∼97, 92, and 90% and a total pore volume of ∼31, 11.5, and 8.6 cm^3/g at the sPS concentration of 0.02, 0.06, and 0.08 g/mL. It is apparent that the pore volume reduced from 31 cm^3/g to 8.6 cm^3/g with a four-fold increase of sPS concentration from 0.02 to 0.08 g/mL. The more open pore structure offered by the gel with 0.02 g/mL sPS is evident from the high-magnification SEM images shown in Figure 4.

The sPS strand diameter is thinnest at 0.02 g/mL of sPS concentration (Figure 4) with the highest specific surface area ∼313 m^2/g compared to 296 m^2/g and 280 m^2/g, respectively, for the sPS gel with 0.06 and 0.08 g/mL concentration (Table 1). The BET adsorption−desorption isotherms for the three sPS aerogels are shown in Figure S5. The meso- and macropore volume fractions of the three sPS aerogels are also quite different. The sPS aerogel produced from the 0.08 g/mL concentration had a mesopore volume fraction of ∼7%, which was the highest among the three aerogels. It is followed by sPS aerogels produced with 0.06 g/mL (5%) and 0.02 g/mL (2%) concentration. Therefore, it is imperative to evaluate the effect of parameters such as the total pore volume, pore size, and specific surface area of the sPS gel on PFOA adsorption performance. The PFOA adsorption experiments were performed by keeping the solid weight of the sPS gel for all three systems constant at 100 mg, allowing the total pore

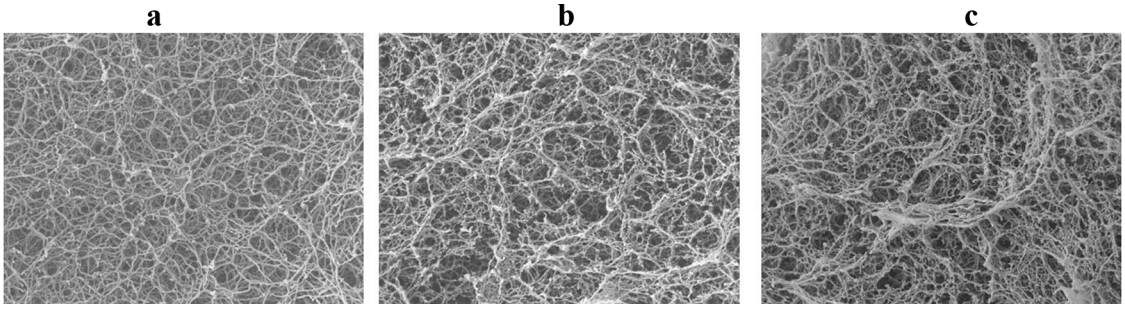

Figure 4. High-magnification SEM images of the sPS aerogel produced with (a) 0.02, (b) 0.06, and (c) 0.08 g/mL concentration of sPS in solution.

https://doi.org/10.1021/acs.langmuir.4c00482
Langmuir 2024, 40, 10208−10216

volume and total BET surface area to play a key role in governing the adsorption behavior.

Figure 5 shows the PFOA adsorption performance of the three sPS wet gels at three different times, i.e., 30, 120, and 300 min. The data clearly indicates that the sPS gel solid concentration played a significant role in determining the rate of adsorption. The sPS gel obtained from the 0.02 g/mL sPS concentration in solution was able to reach ∼84% separation efficiency within 30 min, while the other two gels with a solid concentration of 0.06 and 0.08 g/mL reached separation efficiency values of ∼72 and 32% within the same time. The difference in adsorption performance between the 0.02 and 0.08 g/mL sPS gel was quite large, indicating that parameters such as pore volume, pore size, or specific surface area significantly affected the adsorption process. After 120 min, the 0.02 g/mL sPS gel was able to remove ∼99.2% of PFOA molecules. The sPS gel produced from the 0.06 g/mL sPS concentration needed ∼12 h to reach a 99% separation efficiency.

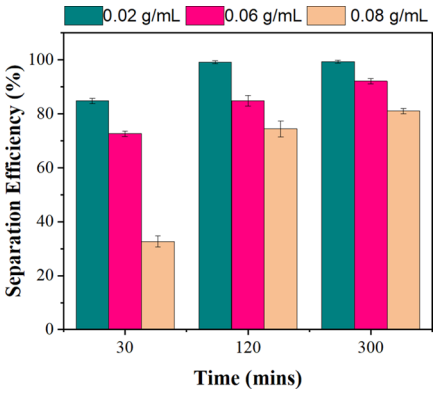

Figure 5. PFOA adsorption by the three different sPS gels of different solid concentrations, 0.02 (green), 0.06 (pink), and 0.08 g/mL (brown) after 30, 120, and 300 min sPS wet gel dimensions: diameter 1.5 ± 0.1 and height 0.85 ± 0.02 cm.

The above trend can be explained as follows. First, the PFOA adsorption kinetics is controlled by the speed of diffusion of PFOA molecules from the bulk to the pores of the sPS wet gel. The wet gel obtained from 0.02 g/mL sPS solution had 97.1% porosity (Table 1) and more abundant open pores (SEM images in Figure 3) compared to 93 and 90% porosity for sPS gels produced from 0.06 and 0.08 g/mL sPS solutions. Thus, the wet gel obtained from 0.02 g/mL sPS allowed faster PFOA diffusion through the tortuous porous network and a greater degree of adsorption of PFOA on sPS strand surfaces with a specific surface area of 313 ± 7 m^2/g (Table 1).

Second, as alluded to earlier in reference to the work of Shin et al.,[49] the PFOA adsorption by the sPS gel is a surface-area driven process. Thus, the gel specimen produced from a 0.02 g/mL sPS solution with a surface area of 313 m^2/g resulted in a higher number of available adsorption sites for PFOA molecules compared to the gels produced from 0.06 and 0.08 g/mL sPS concentration with specific surface areas of 296 and 280 m^2/g, respectively. However, a more thorough study is needed to understand the underlying physics of how the PFOA molecules adsorb onto the sPS surface or interact with each other at the sPS−water interface. It is quite possible that PFOA molecules organized co-operatively on the surfaces of the sPS strand as was observed by Shin et al.[49] in the case of silica and nonionic surfactants. This will be considered in a future investigation.

Extent of Reusability of sPS Gel for PFOA Adsorption. An experiment was performed to test the extent of reusability of the sPS wet gels for removing the PFOA molecules from water until a separation efficiency of less than 90% was observed. This test answered if a gel that adsorbed say 99.98% of PFOA from an industrially relevant concentration in water has more capacity to adsorb PFOA molecules when dipped in a fresh PFOA solution in water. For this purpose, a water-filled sPS gel of 70 mg solid weight produced with a 0.06 g/mL solid concentration was dipped in a 10 mL solution of 1 μg/L PFOA. The gel was allowed to adsorb PFOA molecules for 24 h and subsequently transferred to another 10 mL solution of 1 μg/L PFOA in water. The process was repeated 5 times each time with 24 h adsorption, and the separation efficiency of each step was calculated, as shown in Figure 6. The stepwise efficiency gradually dropped and was reduced to lower than 90% after the fourth cycle. In the first 4 cycles, the separation efficiency was 99.98, 97.98, 92.5, and 90.15%, respectively. This shows the ability of sPS wet gels to adsorb PFOA repeatedly even when the equilibrium adsorption ability of the gel was reached at the end of each step. In this context, conventional adsorbents would not have this ability unless they have extremely high adsorption capacities, which are a result of either a high pore volume or high specific surface areas, but adsorbents with such features are limited. Furthermore, to obtain the maximum adsorption capacity, generally high initial bulk concentrations of PFOA in water are taken (>10−100 mg/L) and the maximum adsorption capacity is taken to be the adsorption value where the curve reaches a plateau in its adsorption performance. It should be noted, however, that the adsorption process is initially concentration-dependent, and hence, starting with a higher concentration would result in a larger number of molecules being adsorbed by the adsorbent. Such a test does not provide a complete picture of what transpires in a real-world situation where the sample is repeatedly subjected to ≤1 μg/L PFOA concentrations. In this regard, the repeated usability of sPS gel, in this study five times, before its separation efficiency dropped to below 90%, allows the adsorbent to be used for longer times without the need for frequent regenerations.

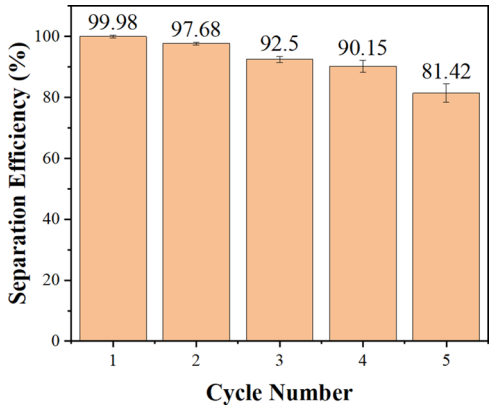

Figure 6. Stepwise separation efficiency of a single sPS gel in a five-step consecutive adsorption process. The PFOA concentration was 1 μg/L in each step. sPS wet gel dimensions: diameter 1.5 ± 0.1 cm and height 0.85 ± 0.02 cm.

https://doi.org/10.1021/acs.langmuir.4c00482
Langmuir 2024, 40, 10208−10216

CONCLUSIONS

The data presented in this work establishes the high separation performance of perfluorooctanoic acid from water at environmentally relevant concentrations using meso- and macroporous syndiotactic polystyrene gels. The sPS wet gels can deplete the concentration of PFOA in water to levels below the EPA's 2024 health advisory limit of 4 ppt. The adsorption kinetics can easily be increased by increasing the pore volume and pore sizes, achieved in this work by varying the % solid content of the gel. A steep rise in the adsorption behavior for PFOA shown by sPS wet gels indicated aggregation of PFOA molecules at the solid−liquid interfaces or within the gel pores. In addition, the high surface area provided by the gel facilitated the reuse of the gel multiple times with a separation efficiency >90%, unlike several low surface area adsorbents such as ion exchange resins, β-cyclodextrin, or microporous activated carbon. In summary, this study demonstrates a novel and promising adsorbent media for the effective removal of PFAS molecules from water.

ASSOCIATED CONTENT

Data Availability Statement

The raw/processed data required to reproduce these findings cannot be shared at this time as the data also forms part of an ongoing study.

Supporting Information

The Supporting Information is available free of charge at https://pubs.acs.org/doi/10.1021/acs.langmuir.4c00482.

Additional data on calibration curve and BET (PDF)

AUTHOR INFORMATION

Corresponding Author

Sadhan C. Jana − *School of Polymer Science and Polymer Engineering, The University of Akron, Akron, Ohio 44325, United States;* orcid.org/0000-0001-8962-380X; Email: janas@uakron.edu

Authors

Pratik S. Gotad − *School of Polymer Science and Polymer Engineering, The University of Akron, Akron, Ohio 44325, United States*

Calum Bochenek − *Department of Chemistry, The University of Akron, Akron, Ohio 44304, United States*

Chrys Wesdemiotis − *School of Polymer Science and Polymer Engineering, The University of Akron, Akron, Ohio 44325, United States; Department of Chemistry, The University of Akron, Akron, Ohio 44304, United States*

Complete contact information is available at: https://pubs.acs.org/10.1021/acs.langmuir.4c00482

Notes

The authors declare no competing financial interest.

ACKNOWLEDGMENTS

This work was partially supported by the ACS Petroleum Research Fund under grant number PRF# 59000-ND7, U.S. National Science Foundation under grant number CMMI 1826030, NSF (DMR-2215940), and industrial members of Coalescence Filtration Nanofibers Consortium at The University of Akron.

REFERENCES

(1) Abbasian Chaleshtari, Z.; Foudazi, R. A Review on Per- and Polyfluoroalkyl Substances (PFAS) Remediation: Separation Mechanisms and Molecular Interactions. *ACS EST Water* **2022**, *2* (12), 2258−2272.

(2) *Avenue, 677 Huntington; Boston; Ma 02115. Stricter federal guidelines on 'forever chemicals' in drinking water pose challenges. News.* https://www.hsph.harvard.edu/news/features/stricter-federal-guidelines-on-forever-chemicals-in-drinking-water-pose-challenges/ (accessed 2023−08−06).

(3) US EPA, O. *EPA Announces New Drinking Water Health Advisories for PFAS Chemicals, $1 Billion in Bipartisan Infrastructure Law Funding to Strengthen Health Protections.* https://www.epa.gov/newsreleases/epa-announces-new-drinking-water-health-advisories-pfas-chemicals-1-billion-bipartisan (accessed 2023−02−08).

(4) *Report: Up to 110 Million Americans Could Have PFAS-Contaminated Drinking Water | EWG.* https://www.ewg.org/research/report-110-million-americans-could-have-pfas-contaminated-drinking-water (accessed 2023-08-06).

(5) Barry, V.; Winquist, A.; Steenland, K. Perfluorooctanoic Acid (PFOA) Exposures and Incident Cancers among Adults Living near a Chemical Plant. *Environ. Health Perspect* **2013**, *121* (11−12), 1313−1318.

(6) Worley, R. R.; Moore, S. M.; Tierney, B. C.; Ye, X.; Calafat, A. M.; Campbell, S.; Woudneh, M. B.; Fisher, J. Per- and Polyfluoroalkyl Substances in Human Serum and Urine Samples from a Residentially Exposed Community. *Environ. Int.* **2017**, *106*, 135−143.

(7) Nayak, S.; Sahoo, G.; Das, I. I.; Mohanty, A. K.; Kumar, R.; Sahoo, L.; Sundaray, J. K. Poly- and Perfluoroalkyl Substances (PFAS): Do They Matter to Aquatic Ecosystems? *Toxics* **2023**, *11* (6), 543.

(8) Brown and Caldwell. *Emerging Contaminants and PFAS.* https://brownandcaldwell.com/services/emerging-contaminants-and-pfas/ (accessed 2023-08-06).

(9) US EPA, O. *EPA and Partners Describe a Chemical Category Prioritization Approach to Select 75 PFAS for Testing using New Approach Methods.* https://www.epa.gov/sciencematters/epa-and-partners-describe-chemical-category-prioritization-approach-select-75-pfas (accessed 2023-08-06).

(10) US EPA, O. *PFAS Chemical Lists and Tiered Testing Methods Descriptions.* https://www.epa.gov/chemical-research/pfas-chemical-lists-and-tiered-testing-methods-descriptions (accessed 2023-08-06).

(11) Chemical & Engineering News. *US EPA sets health advisory limits for 6 PFAS.* https://cen.acs.org/environment/persistent-pollutants/US-EPA-sets-health-advisory-6-PFAS/100/i22 (accessed 2023-08-06).

(12) Podder, A.; Sadmani, A. H. M. A.; Reinhart, D.; Chang, N.-B.; Goel, R. Per and Poly-Fluoroalkyl Substances (PFAS) as a Contaminant of Emerging Concern in Surface Water: A Transboundary Review of Their Occurrences and Toxicity Effects. *Journal of Hazardous Materials* **2021**, *419*, No. 126361.

(13) Xiao, L.; Ling, Y.; Alsbaiee, A.; Li, C.; Helbling, D. E.; Dichtel, W. R. β-Cyclodextrin Polymer Network Sequesters Perfluorooctanoic Acid at Environmentally Relevant Concentrations. *J. Am. Chem. Soc.* **2017**, *139* (23), 7689−7692.

(14) US EPA, O. *Drinking Water Health Advisories for PFOA and PFOS.* https://www.epa.gov/sdwa/drinking-water-health-advisories-pfoa-and-pfos (accessed 2023-08-06).

(15) Bruton, T. A.; Sedlak, D. L. Treatment of Aqueous Film-Forming Foam by Heat-Activated Persulfate Under Conditions Representative of In Situ Chemical Oxidation. *Environ. Sci. Technol.* **2017**, *51* (23), 13878−13885.

(16) OPEC Systems. *In-Situ Treatment: Downhole Foam Fractionation (DFF).* https://opecsystems.com/enviro/pfas-solutions/in-situ-treatment-downhole-foam-fractionation-dff/ (accessed 2023-08-07).

(17) Xiao, F.; Simcik, M. F.; Gulliver, J. S. Mechanisms for Removal of Perfluorooctane Sulfonate (PFOS) and Perfluorooctanoate (PFOA) from Drinking Water by Conventional and Enhanced Coagulation. *Water Res.* **2013**, *47* (1), 49−56.

(18) Woodard, S.; Berry, J.; Newman, B. Ion Exchange Resin for PFAS Removal and Pilot Test Comparison to GAC: WOODARD et Al. *Remediation* **2017**, *27* (3), 19−27.
(19) Flores, C.; Ventura, F.; Martin-Alonso, J.; Caixach, J. Occurrence of Perfluorooctane Sulfonate (PFOS) and Perfluorooctanoate (PFOA) in N.E. Spanish Surface Waters and Their Removal in a Drinking Water Treatment Plant That Combines Conventional and Advanced Treatments in Parallel Lines. *Sci. Total Environ.* **2013**, *461*−*462*, 618−626.
(20) Fagbayigbo, B. O.; Opeolu, B. O.; Fatoki, O. S.; Akenga, T. A.; Olatunji, O. S. Removal of PFOA and PFOS from Aqueous Solutions Using Activated Carbon Produced from Vitis Vinifera Leaf Litter. *Environ. Sci. Pollut Res.* **2017**, *24* (14), 13107−13120.
(21) Xu, J.; Liu, Z.; Zhao, D.; Gao, N.; Fu, X. Enhanced Adsorption of Perfluorooctanoic Acid (PFOA) from Water by Granular Activated Carbon Supported Magnetite Nanoparticles. *Science of The Total Environment* **2020**, *723*, No. 137757.
(22) Park, M.; Wu, S.; Lopez, I. J.; Chang, J. Y.; Karanfil, T.; Snyder, S. A. Adsorption of Perfluoroalkyl Substances (PFAS) in Groundwater by Granular Activated Carbons: Roles of Hydrophobicity of PFAS and Carbon Characteristics. *Water Res.* **2020**, *170*, No. 115364.
(23) Ateia, M.; Alsbaiee, A.; Karanfil, T.; Dichtel, W. Efficient PFAS Removal by Amine-Functionalized Sorbents: Critical Review of the Current Literature. *Environ. Sci. Technol. Lett.* **2019**, *6* (12), 688−695.
(24) Xiao, X.; Ulrich, B. A.; Chen, B.; Higgins, C. P. Sorption of Poly- and Perfluoroalkyl Substances (PFASs) Relevant to Aqueous Film-Forming Foam (AFFF)-Impacted Groundwater by Biochars and Activated Carbon. *Environ. Sci. Technol.* **2017**, *51* (11), 6342−6351.
(25) Karbassiyazdi, E.; Kasula, M.; Modak, S.; Pala, J.; Kalantari, M.; Altaee, A.; Esfahani, M. R.; Razmjou, A. A Juxtaposed Review on Adsorptive Removal of PFAS by Metal-Organic Frameworks (MOFs) with Carbon-Based Materials, Ion Exchange Resins, and Polymer Adsorbents. *Chemosphere* **2023**, *311*, No. 136933.
(26) Teo, N.; Jana, S. C. Solvent Effects on Tuning Pore Structures in Polyimide Aerogels. *Langmuir* **2018**, *34* (29), 8581−8590.
(27) Lin, W.-H.; Jana, S. C. Analysis of Porous Structures of Cellulose Aerogel Monoliths and Microparticles. *Microporous Mesoporous Mater.* **2021**, *310*, No. 110625.
(28) Gotad, P. S.; Kafle, N.; Miyoshi, T.; Jana, S. C. Meso- and Macroporous Polymer Gels for Efficient Adsorption of Block Copolymer Surfactants. *Langmuir* **2022**, *38* (44), 13558−13568.
(29) Mawhinney, K.; Jana, S. C. Design Of Emulsion-Templated Mesoporous−Macroporous Polyurea Gels and Aerogels. *ACS Appl. Polym. Mater.* **2019**, *1* (11), 3115−3129.
(30) Guo, H.; Meador, M. A. B.; McCorkle, L.; Quade, D. J.; Guo, J.; Hamilton, B.; Cakmak, M.; Sprowl, G. Polyimide Aerogels Cross-Linked through Amine Functionalized Polyoligomeric Silsesquioxane. *ACS Appl. Mater. Interfaces* **2011**, *3* (2), 546−552.
(31) Iswar, S.; Galmarini, S.; Bonanomi, L.; Wernery, J.; Roumeli, E.; Nimalshantha, S.; Ben Ishai, A. M.; Lattuada, M.; Koebel, M. M.; Malfait, W. J. Dense and Strong, but Superinsulating Silica Aerogel. *Acta Mater.* **2021**, *213*, No. 116959.
(32) Teo, N.; Jana, S. C. Open Cell Aerogel Foams via Emulsion Templating. *Langmuir* **2017**, *33* (44), 12729−12738.
(33) Kistler, S. S. Coherent Expanded Aerogels and Jellies. *Nature* **1931**, *127* (3211), 741−741.
(34) Baumann, T. F.; Worsley, M. A.; Han, T. Y.-J.; Satcher, J. H. High Surface Area Carbon Aerogel Monoliths with Hierarchical Porosity. *J. Non-Cryst. Solids* **2008**, *354* (29), 3513−3515.
(35) Meador, M. A. B.; Malow, E. J.; Silva, R.; Wright, S.; Quade, D.; Vivod, S. L.; Guo, H.; Guo, J.; Cakmak, M. Mechanically Strong, Flexible Polyimide Aerogels Cross-Linked with Aromatic Triamine. *ACS Appl. Mater. Interfaces* **2012**, *4* (2), 536−544.
(36) Im, H.; Kim, T.; Song, H.; Choi, J.; Park, J. S.; Ovalle-Robles, R.; Yang, H. D.; Kihm, K. D.; Baughman, R. H.; Lee, H. H.; Kang, T. J.; Kim, Y. H. High-Efficiency Electrochemical Thermal Energy Harvester Using Carbon Nanotube Aerogel Sheet Electrodes. *Nat. Commun.* **2016**, *7* (1), 10600.
(37) Aghababaei Tafreshi, O.; Ghaffari-Mosanenzadeh, S.; Karamikamkar, S.; Saadatnia, Z.; Kiddell, S.; Park, B. C.; Naguib, E. H. Novel, Flexible, and Transparent Thin Film Polyimide Aerogels with Enhanced Thermal Insulation and High Service Temperature. *J. Mater. Chem. C* **2022**, *10* (13), 5088−5108.
(38) Teo, N.; Jin, C.; Kulkarni, A.; Jana, S. C. Continuous Fabrication of Core-Shell Aerogel Microparticles Using Microfluidic Flows. *J. Colloid Interface Sci.* **2020**, *561*, 772−781.
(39) Jin, C.; Kulkarni, A.; Teo, N.; Jana, S. C. Fabrication of Pill-Shaped Polyimide Aerogel Particles Using Microfluidic Flows. *Ind. Eng. Chem. Res.* **2021**, *60* (1), 361−370.
(40) Wang, X.; Jana, S. C. Synergistic Hybrid Organic−Inorganic Aerogels. *ACS Appl. Mater. Interfaces* **2013**, *5* (13), 6423−6429.
(41) Lee, D.; Kim, J.; Kim, S.; Kim, G.; Roh, J.; Lee, S.; Han, H. Tunable Pore Size and Porosity of Spherical Polyimide Aerogel by Introducing Swelling Method Based on Spherulitic Formation Mechanism. *Microporous Mesoporous Mater.* **2019**, *288*, No. 109546.
(42) Zhai, C.; Jana, S. C. Tuning Porous Networks in Polyimide Aerogels for Airborne Nanoparticle Filtration. *ACS Appl. Mater. Interfaces* **2017**, *9* (35), 30074−30082.
(43) Baetens, R.; Jelle, B. P.; Gustavsen, A. Aerogel Insulation for Building Applications: A State-of-the-Art Review. *Energy and Buildings* **2011**, *43* (4), 761−769.
(44) Xie, X.; Zheng, Z.; Wang, X.; Lee Kaplan, D. Low-Density Silk Nanofibrous Aerogels: Fabrication and Applications in Air Filtration and Oil/Water Purification. *ACS Nano* **2021**, *15* (1), 1048−1058.
(45) Liang, J.; Wang, Z.; Ye, Q.; Qiao, L.; Jiang, H.; Guo, Y.; Fan, Z. Pump-Inject Antimicrobial and Biodegradable Aerogel as Mask Intermediate Filter Layer for Medical Protection of Air Filtration. *Materials Today Sustainability* **2022**, *19*, No. 100211.
(46) Kim, S. J.; Raut, P.; Jana, S. C.; Chase, G. Electrostatically Active Polymer Hybrid Aerogels for Airborne Nanoparticle Filtration. *ACS Appl. Mater. Interfaces* **2017**, *9* (7), 6401−6410.
(47) Mao, J.; Iocozzia, J.; Huang, J.; Meng, K.; Lai, Y.; Lin, Z. Graphene Aerogels for Efficient Energy Storage and Conversion. *Energy Environ. Sci.* **2018**, *11* (4), 772−799.
(48) Lin, B.; Wang, Z.; Zhu, Q.; Hamzah, W. N. B.; Yao, Z.; Cao, K. Aerogels for the Separation of Asphalt-Containing Oil−Water Mixtures and the Effect of Asphalt Stabilizer. *RSC Adv.* **2020**, *10* (42), 24840−24846.
(49) Shin, T. G.; Müter, D.; Meissner, J.; Paris, O.; Findenegg, G. H. Structural Characterization of Surfactant Aggregates Adsorbed in Cylindrical Silica Nanopores. *Langmuir* **2011**, *27* (9), 5252−5263.
(50) Brumaru, C.; Geng, M. L. Interaction of Surfactants with Hydrophobic Surfaces in Nanopores. *Langmuir* **2010**, *26* (24), 19091−19099.
(51) Samiey, B.; Golestan, S. Adsorption of Triton X-100 on Silica Gel: Effects of Temperature and Alcohols. *cent.eur.j.chem.* **2010**, *8* (2), 361−369.
(52) Shar, J. A.; Obey, T. M.; Cosgrove, T. Adsorption Studies of Polyethers Part 1. Adsorption onto Hydrophobic Surfaces. *Colloids Surf., A* **1998**, *136* (1), 21−33.
(53) Daniel, C.; Alfano, D.; Venditto, V.; Cardea, S.; Reverchon, E.; Larobina, D.; Mensitieri, G.; Guerra, G. Aerogels with a Microporous Crystalline Host Phase. *Adv. Mater.* **2005**, *17* (12), 1515−1518.
(54) Figueroa-Gerstenmaier, S.; Daniel, C.; Milano, G.; Vitillo, J. G.; Zavorotynska, O.; Spoto, G.; Guerra, G. Hydrogen Adsorption by δ and ε Crystalline Phases of Syndiotactic Polystyrene Aerogels. *Macromolecules* **2010**, *43* (20), 8594−8601.
(55) Mancuso, A.; Sacco, O.; Venditto, V.; Navarra, W.; Antico, P.; Daniel, C.; Vaiano, V. Selective Absorption of Aromatic Compounds by Syndiotactic Polystyrene Aerogels. *Macromol. Symp.* **2023**, *408* (1), 2200062.
(56) Kulkarni, A.; Gotad, P.; Joo, P.; Agrawal, A.; Chase, G. C.; Jana, S. C. Water Separation from Diesel Fuel Using High Surface Area 3D-Printed Aerogel Constructs. *Sep. Purif. Technol.* **2024**, *328*, No. 125065.
(57) Joseph, A. M.; Nagendra, B.; Shaiju, P.; Surendran, K. P.; Gowd, E. B. Aerogels of Hierarchically Porous Syndiotactic

Polystyrene with a Dielectric Constant near to Air. *J. Mater. Chem. C* **2018**, *6* (2), 360−368.
(58) Tiberg, F. Physical Characterization of Non-Ionic Surfactant Layers Adsorbed at Hydrophilic and Hydrophobic Solid Surfaces by Time-Resolved Ellipsometry. *Faraday Trans.* **1996**, *92* (4), 531.
(59) Gu, T.; Huang, Z. Thermodynamics of Hemimicellization of Cetyltrimethylammonium Bromide at the Silica Gel/Water Interface. *Colloids Surf.* **1989**, *40*, 71−76.
(60) Lugo, D.; Oberdisse, J.; Karg, M.; Schweins, R.; Findenegg, G. H. Surface Aggregate Structure of Nonionic Surfactants on Silica Nanoparticles. *Soft Matter* **2009**, *5* (15), 2928−2936.
(61) Zhu, B.-Y.; Gu, T. Surfactant Adsorption at Solid-Liquid Interfaces. *Adv. Colloid Interface Sci.* **1991**, *37* (1), 1−32.
(62) Ateia, M.; Attia, M. F.; Maroli, A.; Tharayil, N.; Alexis, F.; Whitehead, D. C.; Karanfil, T. Rapid Removal of Poly- and Perfluorinated Alkyl Substances by Poly(Ethylenimine)-Functionalized Cellulose Microcrystals at Environmentally Relevant Conditions. *Environmental Science & Technology Letters* **2018**, *5*, 764.
(63) Deng, S.; Zhang, Q.; Nie, Y.; Wei, H.; Wang, B.; Huang, J.; Yu, G.; Xing, B. Sorption Mechanisms of Perfluorinated Compounds on Carbon Nanotubes. *Environ. Pollut.* **2012**, *168*, 138−144.
(64) Klemes, M. J.; Ling, Y.; Ching, C.; Wu, C.; Xiao, L.; Helbling, D. E.; Dichtel, W. R. Reduction of a Tetrafluoroterephthalonitrile-β-Cyclodextrin Polymer to Remove Anionic Micropollutants and Perfluorinated Alkyl Substances from Water. *Angew. Chem., Int. Ed.* **2019**, *58* (35), 12049−12053.
(65) Ching, C.; Klemes, M. J.; Trang, B.; Dichtel, W. R.; Helbling, D. E. β-Cyclodextrin Polymers with Different Cross-Linkers and Ion-Exchange Resins Exhibit Variable Adsorption of Anionic, Zwitterionic, and Nonionic PFASs. *Environ. Sci. Technol.* **2020**, *54* (19), 12693−12702.
(66) Inyang, M.; Dickenson, E. R. V. The Use of Carbon Adsorbents for the Removal of Perfluoroalkyl Acids from Potable Reuse Systems. *Chemosphere* **2017**, *184*, 168−175.
(67) Du, Z.; Deng, S.; Bei, Y.; Huang, Q.; Wang, B.; Huang, J.; Yu, G. Adsorption Behavior and Mechanism of Perfluorinated Compounds on Various Adsorbents—A Review. *Journal of Hazardous Materials* **2014**, *274*, 443−454.
(68) Punyapalakul, P.; Suksomboon, K.; Prarat, P.; Khaodhiar, S. Effects of Surface Functional Groups and Porous Structures on Adsorption and Recovery of Perfluorinated Compounds by Inorganic Porous Silicas. *Sep. Sci. Technol.* **2013**, *48*, No. 710888.

https://doi.org/10.1021/acs.langmuir.4c00482
Langmuir 2024, 40, 10208−10216